



# Processor-Efficient Sparse Matrix-Vector Multiplication

L. S. HEATH AND C. J. RIBBENS

Department of Computer Science, Virginia Polytechnic Institute and State University  
Blacksburg, VA 24061-0106, U.S.A.

[heath@cs.vt.edu](mailto:heath@cs.vt.edu) [ribbens@cs.vt.edu](mailto:ribbens@cs.vt.edu)

S. V. PEMMARAJU

Department of Computer Science, The University of Iowa  
Iowa City, IA 52242-1419, U.S.A.

[sriram@cs.uiowa.edu](mailto:sriram@cs.uiowa.edu)

(Received September 2002; revised and accepted June 2003)

**Abstract**—The matrix-vector multiplication operation is the kernel of most numerical algorithms. Typically, matrix-vector multiplication algorithms exploit the sparsity of a matrix, either to reduce the time taken or the memory used. In the case of parallel implementations of numerical algorithms, the sparsity of a matrix can also be used to reduce the number of processing elements (PEs) required. For example, in Leiserson's systolic array algorithm for matrix-vector multiplication the nonzeros in the matrix are partitioned into bands and each band is fed into a different PE. Similarly, in Melhem's algorithm, the nonzeros are partitioned into stripes and each stripe is fed into a distinct PE. However, in many practical applications, such as the numerical solution of partial differential equations, a matrix is much sparser than is indicated by its bandwidth or by its stripe width.

A new measure of sparsity of a matrix called *staircase width* is introduced. A *staircase* in a matrix  $M = (m_{i,j})_{n \times n}$  is a set of matrix positions  $S = \{(i,j) \mid m_{i,j} \neq 0\}$ , such that no position in  $S$  is strictly to the northeast of another position in  $S$ . The *staircase cover* of a matrix is a partition of the positions of nonzero entries in the matrix into staircases and the *staircase width* of a matrix is the size of a smallest staircase cover of the matrix. The staircase width of a matrix is never larger than the bandwidth or the stripe width of a matrix. Moreover, it is significantly smaller than either for some commonly occurring types of matrices such as arrowhead matrices. Experiments with sparse matrices derived from a variety of engineering problems suggest that, in practice, the staircase width of a matrix is about half the stripe width of the matrix. An efficient algorithm to compute a minimum width staircase cover of a matrix is presented. Staircase covers are used as the basis of a new parallel algorithm to compute a matrix-vector product on a linear systolic array of PEs. This algorithm uses as many PEs as the staircase width of the matrix, and therefore, saves on the number of PEs relative to algorithms of Leiserson and Melhem. It is shown that despite using fewer PEs, the algorithm uses no more time steps than Leiserson's or Melhem's algorithm. © 2004 Elsevier Ltd. All rights reserved.

**Keywords**—Bandwidth, Matrix-vector multiplication, Partial orders, Sparse matrices, Staircase width, Stripe width, Systolic arrays.

The authors gratefully acknowledge the support of National Science Foundation Grant CCR-9009953. This research was done while the third author was with the Department of Computer Science, Virginia Polytechnic Institute and State University.

We acknowledge the detailed comments of anonymous referees that has helped make this a better paper.

## 1. INTRODUCTION

Sparse matrix-vector multiplication is an important computational kernel in most scientific computations. Im and Yelick [1,2] mention signal and image processing, document retrieval, and data mining as some of the applications in which efficient sparse matrix-vector multiplication is critical. Matrix-vector multiplication is often used in iterative solvers for linear systems, in explicit methods for ordinary differential equations, and in eigenvalue computations [1,3]. In general, the performance of sparse matrix operations is much lower than their dense matrix counterparts. This is mainly because the memory access patterns are irregular and there is an overhead for manipulating the sparse matrix representation. Sparsity of a matrix is a problem for parallel implementations as well and implementations that work well for dense matrices often expend a large fraction of their computational resources performing unnecessary operations that involve zeros.

Given that the matrices used in most practical applications are sparse, attempts to exploit the sparsity of matrices to speed up matrix computations continue. Exploitation of sparsity typically involves symbolic preprocessing of a matrix based on its sparsity structure [4]. The preprocessing may yield a decomposition of the sparse matrix that can then be processed with a specialized algorithm. Sometimes the decomposition leads to a number of smaller dense matrix subproblems, which can then be solved with a system for dense linear algebra, such as BLAS [5] or LAPACK [5,6]. Some of the important measures or techniques associated with sparsity are matrix bandwidth [7,8]; matrix stripe width [3,9]; block matrices [10,11]; the jagged diagonal data structure [12]; frontal and multifrontal methods [13,14]; and panel clustering [15,16].

Melhem [3,9] introduced a systolic array network for performing matrix-vector multiplications and solving triangular systems of equations. In Melhem's scheme, the processing elements (PEs) in the systolic array avoid many unnecessary operations, while the number of PEs utilized is small. The basis of Melhem's scheme is a decomposition of the nonzero elements of the matrix into stripes. Each stripe is fed into a different PE, and therefore, Melhem's scheme utilizes only as many PEs as the number of stripes required to cover the matrix. Melhem [3] mentions that, in matrices that arise in finite-element analysis, the bandwidth of an  $n \times n$  matrix is typically  $\Theta(n^{1/2})$  (for 2-D problems) or  $\Theta(n^{2/3})$  (for 3-D problems), while the number of stripes required to cover the matrix is bounded above by a constant (independent of  $n$ ). Therefore, as compared with the scheme described by Leiserson [17], which uses as many PEs as the bandwidth of a matrix, Melhem's scheme uses far fewer PEs in application domains such as finite-element analysis.

In this paper, we introduce a new way of imposing structure on sparse matrices, called *staircase covers*. The notion of staircase covers generalizes the notion of stripe covers, used by Melhem. We then present a new matrix-vector multiplication algorithm on systolic arrays that uses as many PEs as the number of staircases required to cover the matrix. We show that the minimum number of staircases required to cover a matrix is never greater than the minimum number of stripes required. Furthermore, in matrices such as arrowhead matrices that arise in various engineering applications, the number of staircases required to cover the matrix is bounded above by a constant, whereas the number of stripes required is  $\Theta(n)$  for an  $n \times n$  matrix. Section 4 describes experiments in which the sizes of minimum staircase covers and stripe covers are computed for a number of sparse matrices that arise in engineering applications. Experiments indicate that the average number of stripes required to cover a matrix is about two times the number of staircases required. Finally, we show that this saving in the number of PEs required by our scheme is achieved *without* using any additional time steps as compared to Melhem's algorithm.

As in Leiserson's and Melhem's algorithms, the amount of hardware required by our algorithm depends on the sparsity structure of the matrix and this is only known at runtime. There are two reasons why this is not a significant concern. First, reconfigurable VLSI technology [18], especially in the form of field-programmable gate arrays (FPGAs), is capable of being *reconfigured dynamically* to provide the resources necessary to implement a systolic array having any number

of virtual processors [19–22]. FPGAs can even be connected with buses in parallel, so there are few limits on how much hardware can be made available [23,24]. Second, our scheme is sufficiently flexible that a smaller number of PEs can be adapted through partitioning the set of staircases in a staircase cover, feeding each subset into the PEs, and accumulating the results.

## 2. PRELIMINARIES

Throughout the paper, we use  $M = (m_{i,j})_{n \times n}$  to denote an  $n \times n$  matrix with entries  $m_{i,j}$  and use  $x = (x_j)_{n \times 1}$  to denote an  $n$ -vector with entries  $x_j$ . Let  $J_n = \{1, 2, \dots, n\}$  be the set of row (or column) indices of  $M$ . Each ordered pair  $(i, j) \in J_n^2$  is a *position index* of  $M$ . The position index  $(i, j)$  is said to *cover* the corresponding entry  $m_{i,j}$  of  $M$ . Let  $\Gamma \subseteq J_n^2$  be the set of position indices that cover nonzero entries of  $M$ ; that is,  $\Gamma = \{(i, j) \in J_n^2 \mid m_{i,j} \neq 0\}$ . *Diagonal  $k$*  of  $M$  is the set of position indices  $D_k = \{(i, j) \in J_n^2 \mid j - i = k\}$ . The *band* of  $M$  is the smallest contiguous set of diagonals  $\{D_p, D_{p+1}, \dots, D_q\}$  that covers  $\Gamma$ ; the *bandwidth*  $\text{BAND}(M)$  of  $M$  is  $q - p + 1$ , the cardinality of its band. Figure 1 illustrates a pattern of nonzero entries (black squares) in a  $5 \times 5$  matrix. The matrix has bandwidth 5, and the leftmost drawing shows its nonzero entries covered by five bands. Leiserson [17] proposes a systolic array for multiplying a matrix  $M$  of bandwidth  $b = \text{BAND}(M)$  and a vector  $x$  using a linear array of  $b$  PEs, requiring  $2n + b$  clock beats to accomplish the multiplication.

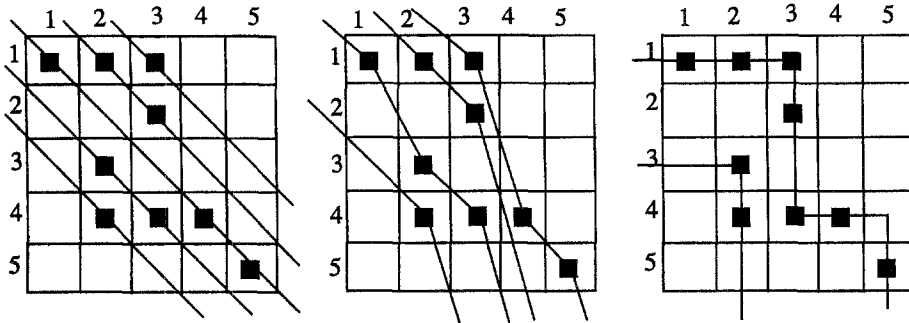


Figure 1. A matrix with bandwidth 5, stripe width 4, and staircase width 2.

In many practical applications, such as finite-element analysis,  $M$  is much sparser than is indicated by its bandwidth. Melhem [3] proposed a systolic network called MAT/VEC to take advantage of such sparsity. To describe MAT/VEC and our scheme in the same framework, we introduce some terminology related to partial orders (see [25]). A *partial order* is a binary relation that is reflexive, antisymmetric, and transitive. A *partially ordered set* (poset)  $P = (S, \leq)$  is a set  $S$  with a partial order  $\leq$  defined on it. For a pair of elements,  $s, s' \in S$ , we say  $s < s'$  if  $s \leq s'$  and  $s \neq s'$ . A set of elements  $\{s_1, s_2, \dots, s_k\}$  from  $S$ , such that  $s_i \leq s_{i+1}$ , where  $1 \leq i \leq k - 1$ , is called a *chain* in  $P$ . The *length* of a chain is simply the number of elements in it. An *antichain* in a poset  $P = (S, \leq)$  is a subset  $S' \subseteq S$ , such that no two elements in  $S'$  are related by  $\leq$ . Suppose that  $S' \subseteq S$  and  $s \in S'$ . Then  $s$  is a maximal element of  $S'$  if, for every  $s' \in S'$ , either  $s' \leq s$  or  $s$  and  $s'$  are unrelated by  $\leq$ . Similarly,  $s$  is a minimal element of  $S'$  if, for every  $s' \in S'$ , either  $s \leq s'$  or  $s$  and  $s'$  are unrelated by  $\leq$ .

Define the *strictly southeast poset*  $(\Gamma, \leq_{\text{sse}})$  by  $(i_1, j_1) \leq_{\text{sse}} (i_2, j_2)$  if either  $(i_1, j_1) = (i_2, j_2)$  or  $i_1 < i_2$  and  $j_1 < j_2$ . A *stripe*  $\Upsilon \subseteq \Gamma$  in  $M$  is a nonempty chain in the poset  $(\Gamma, \leq_{\text{sse}})$ ; stripes are generalizations of diagonals. A *stripe cover* of  $M$  is a set of stripes that covers the set of nonzero entries  $\Gamma$ . The *stripe width*  $\text{STRIPE}(M)$  is the minimum cardinality of any stripe cover of  $M$ . For example, the matrix in Figure 1 has stripe width 4, and the middle drawing shows its nonzeros covered by four stripes. The nonzero entries  $(1, 3)$ ,  $(2, 3)$ ,  $(3, 2)$ , and  $(4, 2)$  have to belong to distinct stripes, and hence, four is the fewest number of stripes required. The optimal

stripe cover shown in Figure 1 is

$$\{(1, 3), (4, 4), (5, 5)\}, \{(1, 2), (2, 3)\}, \{(1, 1), (3, 2), (4, 3)\}, \{(4, 2)\}.$$

It is easy to see that a band of  $M$  is also a stripe cover of  $M$ , and hence, the stripe width of  $M$  is no greater than its bandwidth.

Define the *southeast poset*  $(\Gamma, \leq_{\text{se}})$  by  $(i_1, j_1) \leq_{\text{se}} (i_2, j_2)$  if and only if  $i_1 \leq i_2$  and  $j_1 \leq j_2$ . A *staircase*  $\Psi \subseteq \Gamma$  in  $M$  is a nonempty chain in the poset  $(\Gamma, \leq_{\text{se}})$ . A *staircase cover* of  $M$  is a set of staircases that covers  $\Gamma$ . The *staircase width*  $\text{STAIR}(M)$  is the minimum cardinality of any staircase cover of  $M$ . For example, the matrix in Figure 1 has staircase width 2, and the rightmost drawing shows its nonzeros covered by two staircases. The nonzero entries  $(3, 2)$  and  $(2, 3)$  have to belong to different staircases, and therefore, two is the fewest number of staircases required. The optimal staircase cover shown in Figure 1 is

$$\{(1, 1), (1, 2), (1, 3), (2, 3), (4, 3), (4, 4), (5, 5)\}, \{(3, 2), (4, 2)\}.$$

A stripe is also a staircase, and hence, the staircase width of a matrix is no greater than its stripe width. To multiply the matrix in Figure 1 with any 5-vector, Leiserson's systolic array requires five PEs, Melhem's MAT/VEC requires four PEs, while our scheme requires two PEs.

This paper's contributions can be summarized as follows.

1. In Section 3, we show how to efficiently compute an optimal staircase cover of a matrix. Our algorithm takes a list of the position indices of  $m$  nonzero elements in an  $n \times n$  matrix as input and has time complexity  $O(m \log \log n)$ .
2. In Sections 5 and 6, we present a new systolic array algorithm for matrix-vector multiplication called the *generalized MAT/VEC*. As MAT/VEC does with stripes, generalized MAT/VEC feeds the nonzero entries covered by each staircase to a corresponding PE. Thus, generalized MAT/VEC can perform the multiplication with as many PEs as  $\text{STAIR}(M)$ .
3. Since the staircase width of a matrix is never greater than, and in many applications significantly smaller than, the stripe width of the matrix, generalized MAT/VEC saves on PEs relative to MAT/VEC. In Section 4, we describe experiments in which we have computed the bandwidth, stripe width, and staircase width of sparse matrices that arise from a variety of applications, for example, fluid mechanics, financial portfolio optimization, structural engineering, and linear programming. For these matrices, the average value of  $\text{STRIPE}(M)$  is more than two times the average value of  $\text{STAIR}(M)$ .
4. In Section 7, we show that, even though generalized MAT/VEC saves on PEs as compared to MAT/VEC, it does not require additional time steps. Using Melhem's notion of *global cycles*, we show that generalized MAT/VEC and MAT/VEC perform the same computations in each global cycle, and thus, take exactly the same number of global cycles to perform a matrix-vector multiplication (Theorem 8). Thus, generalized MAT/VEC achieves a savings in hardware without requiring additional time steps.

### 3. COMPUTING A STAIRCASE COVER

In Section 5, we describe generalized MAT/VEC and show that its correctness depends on a staircase cover of matrix  $M$  in which the staircases are totally ordered in a sense that will be made precise in the following. In this section, we sketch an algorithm that computes an optimal staircase cover of  $M$  that is totally ordered as required by generalized MAT/VEC. First, we present an alternate characterization of the staircase width of a matrix. Then we define a partial order  $\leq_\gamma$  on the set of all staircases of  $M$ .

Define the *northeast poset*  $(\Gamma, \leq_{\text{ne}})$  by  $(i_1, j_1) \leq_{\text{ne}} (i_2, j_2)$  if and only if  $i_1 \geq i_2$  and  $j_1 \leq j_2$ . Define the *strictly northeast poset*  $(\Gamma, \leq_{\text{sne}})$  by  $(i_1, j_1) \leq_{\text{sne}} (i_2, j_2)$  if and only if either  $(i_1, j_1) =$

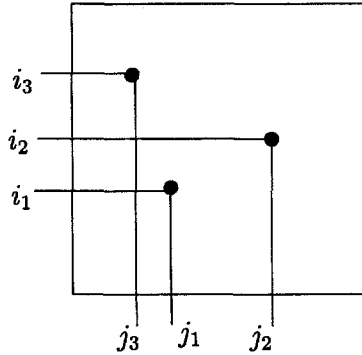


Figure 2. Illustrating the posets  $\leq_{ne}$  and  $\leq_{se}$ . Here  $(i_1, j_1) \leq_{ne} (i_2, j_2)$  and  $(i_1, j_1) \leq_{sne} (i_2, j_2)$ . Also,  $(i_3, j_3) \leq_{se} (i_2, j_2)$  and  $(i_3, j_3) \leq_{sse} (i_2, j_2)$ .

---

```

 $S_0 := \Gamma;$ 
 $\ell := 1;$ 
while  $(S_{\ell-1} \neq \emptyset)$  do
    let  $\Psi_\ell$  be the set of maximal elements in  $(S_{\ell-1}, \leq_{sne});$ 
     $S_\ell := S_{\ell-1} - \Psi_\ell;$ 
     $\ell := \ell + 1;$ 
endwhile;
return  $\Psi_1, \Psi_2, \dots, \Psi_{\ell-1}$ 

```

---

Figure 3. Staircase Cover Algorithm (SCA).

$(i_2, j_2)$  or  $i_1 > i_2$  and  $j_1 < j_2$ . Figure 3 illustrates the various posets we have defined. An *antistaircase* in  $M$  is a chain in the poset  $(\Gamma, \leq_{sne})$ . Using the following well-known theorem of Dilworth, we obtain an alternate characterization of the staircase width of  $M$ .

**THEOREM 1.** (See [26].) *Let  $P = (S, \leq)$  be a finite poset. The minimum number of chains required to cover all the elements of  $S$  equals the size of the largest antichain in  $P$ .*

The following corollary to Dilworth's theorem provides a characterization of the staircase width of a matrix.

**LEMMA 2.** *The size of the largest antistaircase in  $\Gamma$  equals  $\text{STAIR}(M)$ .*

**PROOF.** We first claim that a subset of  $\Gamma$  is an antistaircase in  $M$  if and only if it is an antichain in the poset  $(\Gamma, \leq_{se})$ . To see this, consider an arbitrary antistaircase in  $M$ ,  $\{(i_1, j_1), (i_2, j_2), \dots, (i_k, j_k)\}$ . By definition, this is a chain in  $\leq_{sne}$ , and therefore, without loss of generality we have

$$i_1 > i_2 > \dots > i_k \quad \text{and} \quad j_1 < j_2 < \dots < j_k.$$

From this it follows that for any pair of position indices  $(i_p, j_p)$  and  $(i_q, j_q)$ ,  $(i_p, j_p) \not\leq_{se} (i_q, j_q)$  and  $(i_q, j_q) \not\leq_{se} (i_p, j_p)$ . Therefore,  $\{(i_1, j_1), (i_2, j_2), \dots, (i_k, j_k)\}$  is an antichain in the poset  $(\Gamma, \leq_{se})$ . The argument that proves the converse is similar.

Thus, a largest antistaircase in  $\Gamma$  is a largest antichain in the poset  $(\Gamma, \leq_{se})$ .  $\text{STAIR}(M)$  is the minimum number of chains in the poset  $(\Gamma, \leq_{se})$  required to cover  $\Gamma$ . By Theorem 1 the lemma follows.  $\blacksquare$

For the matrix shown in Figure 1 there are several largest antistaircases;  $\{(3, 2), (2, 3)\}$  and  $\{(3, 2), (1, 3)\}$  are two examples. From the lemma, it follows that the staircase width of the matrix is 2.

We now define binary relations  $\leq_\gamma$  and  $<_\gamma$  on the set of all staircases in  $M$ . For a pair of staircases  $\Psi_1$  and  $\Psi_2$  in  $M$ ,  $\Psi_2 <_\gamma \Psi_1$  if both  $\Psi_1 \cap \Psi_2 = \emptyset$  and, for every position index  $(i_2, j_2) \in \Psi_2$ ,

there is a position index  $(i_1, j_1) \in \Psi_1$ , such that  $(i_2, j_2) <_{\text{sne}} (i_1, j_1)$ . Define  $\Psi_2 \leq_\gamma \Psi_1$ , if either  $\Psi_2 <_\gamma \Psi_1$  or  $\Psi_2 = \Psi_1$ . As we show in the following lemma,  $\leq_\gamma$  defines a partial order on the set of all staircases in  $M$ .

LEMMA 3.  $\leq_\gamma$  is a partial order on the set of all staircases of  $M$ .

PROOF. By definition,  $\leq_\gamma$  is reflexive. It suffices to show that  $<_\gamma$  is antisymmetric and transitive. To show that  $<_\gamma$  is antisymmetric, consider staircases  $\Psi_1, \Psi_2$ , such that  $\Psi_2 <_\gamma \Psi_1$ . Suppose  $(i_2, j_2) \in \Psi_2$ . By definition of  $<_\gamma$ , there exists  $(i_1, j_1) \in \Psi_1$ , such that  $(i_2, j_2) <_{\text{sne}} (i_1, j_1)$ . Now suppose  $\Psi_1 <_\gamma \Psi_2$ . Then, there exists  $(i_3, j_3) \in \Psi_2$ , such that  $(i_1, j_1) <_{\text{sne}} (i_3, j_3)$ . By transitivity of  $<_{\text{sne}}$ , we have  $(i_2, j_2) <_{\text{sne}} (i_3, j_3)$ . But, this is a contradiction to  $(i_2, j_2)$  and  $(i_3, j_3)$  belonging to the same staircase.

To show that  $<_\gamma$  is transitive, consider staircases  $\Psi_1, \Psi_2$ , and  $\Psi_3$ , such that  $\Psi_3 <_\gamma \Psi_2$  and  $\Psi_2 <_\gamma \Psi_1$ . Suppose  $(i_3, j_3) \in \Psi_3$ . By definition of  $<_\gamma$ , there exists  $(i_2, j_2) \in \Psi_2$ , such that  $(i_3, j_3) <_{\text{sne}} (i_2, j_2)$ . Also by definition, there exists  $(i_1, j_1) \in \Psi_1$ , such that  $(i_2, j_2) <_{\text{sne}} (i_1, j_1)$ . Transitivity of  $<_{\text{sne}}$  implies that  $(i_3, j_3) <_{\text{sne}} (i_1, j_1)$ . Since  $(i_3, j_3)$  was arbitrary, we conclude that for every  $(i_3, j_3) \in \Psi_3$  there exists  $(i_1, j_1) \in \Psi_1$ , such that  $(i_3, j_3) <_{\text{sne}} (i_1, j_1)$ . Hence,  $\Psi_3 <_\gamma \Psi_1$ , as desired. ■

For the purposes of generalized MAT/VEC, we are interested in a staircase cover of  $M$  that is totally ordered by  $\leq_\gamma$ . The proof of the following theorem includes an algorithm for constructing such a staircase cover of  $M$ .

THEOREM 4. Every matrix  $M$  has a staircase cover consisting of STAIR( $M$ ) staircases that are totally ordered by  $\leq_\gamma$ .

PROOF. The proof uses an algorithm that we call the *staircase cover algorithm* (SCA) (see Figure 3). SCA takes a matrix  $M$  as input and returns a set of nonempty sets of position indices

$$\Pi = \{\Psi_1, \Psi_2, \dots, \Psi_k\}.$$

We show that  $\Pi$  constitutes an optimal staircase cover of  $M$  and that  $\Psi_\ell <_\gamma \Psi_{\ell-1}$  for all  $\ell$ ,  $2 \leq \ell \leq k$ . These properties are established in the following three steps.

1.  $\Pi$  is a staircase cover of  $M$ . By definition of maximal elements, if  $(i_1, j_1), (i_2, j_2) \in \Psi_\ell$  are distinct position indices, then neither  $(i_1, j_1) \leq_{\text{sne}} (i_2, j_2)$  nor  $(i_2, j_2) \leq_{\text{sne}} (i_1, j_1)$ . Hence, either  $(i_1, j_1) \leq_{\text{se}} (i_2, j_2)$  or  $(i_2, j_2) \leq_{\text{se}} (i_1, j_1)$ . As every pair of elements of  $\Psi_\ell$  are related by  $\leq_{\text{se}}$ , we have that  $\Psi_\ell$  is a chain in  $(\Gamma, \leq_{\text{se}})$ . Thus,  $\Psi_\ell$  is a staircase in  $M$ . After  $\ell$  times through the while-do loop in SCA,

$$\Gamma = \Psi_1 \cup \Psi_2 \cup \dots \cup \Psi_\ell \cup S_\ell.$$

When SCA terminates,  $S_k = \emptyset$ . Hence,  $\{\Psi_1, \Psi_2, \dots, \Psi_k\}$  is a staircase cover of  $M$ .

2.  $\Pi$  is an optimal staircase cover. For an arbitrary element  $(i_k, j_k) \in \Psi_k$ , there exists at least one element  $(i_{k-1}, j_{k-1}) \in \Psi_{k-1}$ , such that  $(i_k, j_k) <_{\text{sne}} (i_{k-1}, j_{k-1})$ . Otherwise,  $(i_k, j_k)$  would have been included in  $\Psi_{k-1}$ . Extending this argument inductively, it is easy to see that there exists a sequence of position indices

$$(i_k, j_k) <_{\text{sne}} (i_{k-1}, j_{k-1}) <_{\text{sne}} \dots <_{\text{sne}} (i_1, j_1),$$

such that  $(i_\ell, j_\ell) \in \Psi_\ell \subseteq \Gamma$  for all  $\ell$ ,  $1 \leq \ell \leq k$ . This implies that there is an antistaircase of size  $k$  in  $\Gamma$ . Applying Lemma 2, we conclude that  $\{\Psi_1, \Psi_2, \dots, \Psi_k\}$  is an optimal staircase cover of  $M$ .

3.  $\leq_\gamma$  is a total order on  $\Pi$ . Consider an arbitrary pair of staircases  $\Psi_r$  and  $\Psi_{r+1}$  in  $\Pi$ , where  $1 \leq r \leq k-1$ . As mentioned in the proof of Property 2, for any position index  $(i, j) \in \Psi_{r+1}$ , there exists a position index  $(i', j') \in \Psi_r$ , such that  $(i, j) <_{\text{sne}} (i', j')$ . Hence,  $\Psi_{r+1} <_\gamma \Psi_r$ . ■

The application of SCA to the nonzeros of Figure 1 yields these two staircases

$$\begin{aligned}\Psi_1 &= \{(1, 1), (1, 2), (1, 3), (2, 3), (4, 3), (4, 4), (5, 5)\}, \\ \Psi_2 &= \{(3, 2), (4, 2)\},\end{aligned}$$

also illustrated in the rightmost picture in Figure 1. Note that  $\Psi_1$  consists of the maximal elements of  $(\Gamma, \leq_{\text{sne}})$ , as for each  $(i, j) \in \Psi_1$ , there is no  $(i', j') \in \Gamma$  that is strictly north and east of it. Note that there are other optimal staircase covers of the matrix in Figure 1 that are not totally ordered by  $\leq_\gamma$ . One example of such a staircase cover is

$$\{\{(1, 1), (1, 2), (1, 3), (2, 3)\}, \{(3, 2), (4, 2), (4, 3), (4, 4), (5, 5)\}\}.$$

The notion of a staircase in a matrix is equivalent to the notion of a queue layout of a graph [27–31]. In particular, the queue layout of a graph corresponds to a staircase cover of the adjacency matrix of the graph and finding the minimum number of queues for a particular layout of a graph is equivalent to computing the staircase width of the corresponding adjacency matrix. Reference [31] presents an algorithm for determining the fewest queues required for a graph layout that runs in  $O(m \log \log n)$  time on a graph with  $n$  vertices and  $m$  edges. With minor modifications, this algorithm can also be used to implement SCA in  $O(|\Gamma| \log \log n)$  time on an  $n \times n$  matrix, where  $\Gamma$  is the set of positions of nonzero entries in the matrix. The assumption here is that  $\Gamma$  is the input to the algorithm.

In the context of our application of staircase covers to matrix-vector multiplication on systolic arrays, a *systolic algorithm* to compute a minimum width staircase cover of a matrix may be useful. This is beyond the scope of the current paper, but we suspect that techniques traditionally used for sorting on systolic arrays (see [32] for an example) will be useful in computing staircase covers as well.

#### 4. COMPARING BANDWIDTH, STRIPE WIDTH, AND STAIRCASE WIDTH

As mentioned in Section 2, for any matrix  $M$ , the following inequality holds:

$$\text{BAND}(M) \geq \text{STRIPE}(M) \geq \text{STAIR}(M).$$

It is of course good news for generalized MAT/VEC that  $\text{STRIPE}(M) \geq \text{STAIR}(M)$  for all matrices  $M$ , but the important question is how much smaller is the staircase width as compared to stripe width for the kinds of sparse matrices that arise in real applications. In this section, we describe experiments that show that for sparse matrices derived for a variety of applications, we can expect  $\text{STRIPE}(M)$  to be about twice the size of  $\text{STAIR}(M)$ . Furthermore, these experiments show there are matrices that arise in real applications for which the staircase width is dramatically smaller than the stripe width.

For our experiments we downloaded 25 real, nonsymmetric matrices from the University of Florida sparse matrix collection, which currently contains 926 sparse matrices that have arisen in a variety of real applications<sup>1</sup>. These matrices are all stored in the popular Harwell/Boeing format. To complete our experiments in a reasonable amount of time, we restricted our sample to matrices with 5000 or fewer rows and columns. The matrices in the University of Florida collection are organized into directories, each directory containing matrices submitted by a research group. Roughly speaking, this organization partitions matrices into directories by problem domain. Therefore, to prevent any bias and to get matrices from a wide variety of problem domains, we considered the matrix directories in alphabetical order and selected up to two

<sup>1</sup>This collection can be found at <http://www.cise.ufl.edu/research/sparse/matrices/>.

matrices satisfying our criteria (real, nonsymmetric, number of rows, columns  $\leq 5000$ ) from each directory. Within each matrix directory, we selected the first two matrices in alphabetical order that satisfy our criteria. (While our programs to compute bandwidth, stripe width, and staircase width work for nonsquare matrices also, all the matrices selected in this manner, turned out to be square.) Our programs, data files, and documentation are all available at <http://www.cs.uiowa.edu/~sriram/sparseMatrices/experiments.html/>.

The results of our experiments are shown in the table in Figure 4. The second column gives the directory and file name of the matrix, as found at <ftp://ftp.cise.ufl.edu/pub/faculty/davis/matrices/>. The average sparsity of a matrix is more than 96%, so these matrices are quite sparse. The last three columns show the staircase width (SCW), stripe width (SW), and bandwidth (BW) computed by the programs available at the URL given above.

|    | File name            | Dimensions         | Nonzeros | Sparsity | SCW   | SW     | BW      |
|----|----------------------|--------------------|----------|----------|-------|--------|---------|
| 1  | Bai/bfwa398.rua      | 398 $\times$ 398   | 3678     | 97.68    | 20    | 32     | 609     |
| 2  | Bai/bfwa62.rua       | 62 $\times$ 62     | 450      | 88.29    | 15    | 28     | 99      |
| 3  | Brethour/coater1.rua | 1348 $\times$ 1348 | 19457    | 98.93    | 57    | 137    | 869     |
| 4  | DRIVCAV/cavity01.rua | 317 $\times$ 317   | 7327     | 92.71    | 33    | 105    | 205     |
| 5  | DRIVCAV/cavity02.rua | 317 $\times$ 317   | 7327     | 92.71    | 33    | 108    | 205     |
| 6  | FIDAP/ex1.rua        | 216 $\times$ 216   | 4352     | 90.67    | 34    | 79     | 129     |
| 7  | FIDAP/ex10.rua       | 2410 $\times$ 2410 | 54840    | 99.06    | 33    | 53     | 227     |
| 8  | Garon/garon1.rua     | 3175 $\times$ 3175 | 88927    | 99.12    | 60    | 127    | 6343    |
| 9  | Grund/b1_ss.rua      | 7 $\times$ 7       | 15       | 69.39    | 3     | 4      | 10      |
| 10 | Grund/b2_ss.rua      | 1089 $\times$ 1089 | 4228     | 99.64    | 260   | 387    | 2017    |
| 11 | HB/arc130.rua        | 130 $\times$ 130   | 1282     | 92.41    | 23    | 206    | 251     |
| 12 | HB/bp_0.rua          | 822 $\times$ 822   | 3276     | 99.52    | 41    | 267    | 1337    |
| 13 | Hamm/add20.rua       | 2395 $\times$ 2395 | 17319    | 99.70    | 86    | 232    | 4627    |
| 14 | Hamm/add32.rua       | 4960 $\times$ 4960 | 23884    | 99.90    | 32    | 84     | 8059    |
| 15 | Mallya/lhr01.rua     | 1477 $\times$ 1477 | 18592    | 99.15    | 72    | 223    | 2537    |
| 16 | Mallya/lhr02.rua     | 2954 $\times$ 2954 | 37206    | 99.58    | 72    | 223    | 2537    |
| 17 | Shyy/shyy41.rua      | 4720 $\times$ 4720 | 20042    | 99.91    | 4     | 6      | 81      |
| 18 | Simon/raefsky1.rua   | 3242 $\times$ 3242 | 294276   | 97.20    | 111   | 320    | 871     |
| 19 | Simon/raefsky2.rua   | 3242 $\times$ 3242 | 294276   | 97.20    | 111   | 320    | 871     |
| 20 | TOKAMAK/utm1700b.rua | 1700 $\times$ 1700 | 21509    | 99.26    | 24    | 43     | 512     |
| 21 | TOKAMAK/utm300.rua   | 300 $\times$ 300   | 3155     | 96.50    | 23    | 41     | 141     |
| 22 | Wang/swang1.rua      | 3169 $\times$ 3169 | 20841    | 99.79    | 58    | 108    | 6127    |
| 23 | Wang/swang2.rua      | 3169 $\times$ 3169 | 20841    | 99.79    | 58    | 108    | 6127    |
| 24 | Zitney/extr1.rua     | 2837 $\times$ 2837 | 11407    | 99.86    | 913   | 1136   | 5318    |
| 25 | Zitney/radfr1.rua    | 1048 $\times$ 1048 | 13299    | 98.79    | 15    | 33     | 1075    |
|    | Means                |                    |          | 96.27    | 87.64 | 187.92 | 2047.36 |
|    | Medians              |                    |          | 99.06    | 34    | 108    | 871     |

Figure 4. The staircase width (SCW), stripe width (SW), and the bandwidth (BW) of 25 real, nonsymmetric matrices is shown here. These matrices were downloaded from the University of Florida sparse matrix collection.

It is easy to construct examples of  $n \times n$  matrices whose bandwidth is  $\Theta(n)$  and whose stripe width is  $O(1)$ . For example, consider the  $n \times n$  matrix  $M$ , with even  $n$ , such that

$$\Gamma = \{(1, 1), (2, 3), (3, 5), \dots, (n/2, n - 1)\}.$$

Then,  $\text{STRIPE}(M) = 1$  but the bandwidth of  $M$  is  $n/2$ . More to the point, Melhem mentions that in matrices that arise in finite-element analysis, the bandwidth of an  $n \times n$  matrix is typ-



ically  $\Theta(n^{1/2})$  (for 2-D problems) or  $\Theta(n^{2/3})$  (for 3-D problems), while the number of stripes required to cover the matrix is bounded above by a constant (independent of  $n$ ). These observations are supported by our experiments. In the table in Figure 4, the average stripe width is 187.92, while the average bandwidth is 2047.46. For several matrices in the table, the difference between the stripe width and bandwidth is even more dramatic. For example, the average bandwidth of the three matrices `garon1.rua` (Row 8), `add32.rua` (Row 14), and `swang1.rua` (Row 22) is 6843, more than 60 times the average stripe width, which is 106.3. The matrices `garon1.rua` and `swang1.rua` arise from 2-D and 3-D finite-element discretization of the Navier-Stokes equation, whereas `add32.rua` arises in digital circuit simulation. Figure 5 shows the patterns of nonzeros in these matrices, and these patterns explain why it requires many bands to cover the nonzeros but very few stripes.

The difference in the average values of stripe width and staircase width is not as dramatic as the difference between the stripe width and bandwidth. Nevertheless, the average stripe width is about twice the average staircase width. The matrix `arc130.rua` is an example in which the stripe width is dramatically larger than the staircase width. Figure 6 shows the pattern of nonzeros in this matrix and from the picture it is clear that the nonzeros have an arrowhead pattern. Matrices with this nonzero pattern occur frequently in the numerical solution to partial differential equations and there are papers that focus on efficient matrix operations for arrowhead matrices [33].

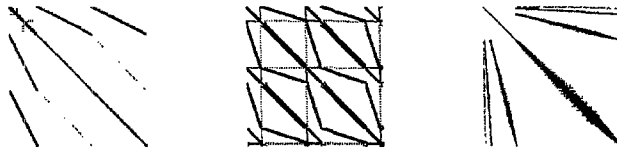


Figure 5. The pattern of nonzeros in the matrices `garon1.rua` ( $3175 \times 3175$ ), `add32.rua` ( $4960 \times 4960$ ), and `swang1.rua` ( $3169 \times 3169$ ).

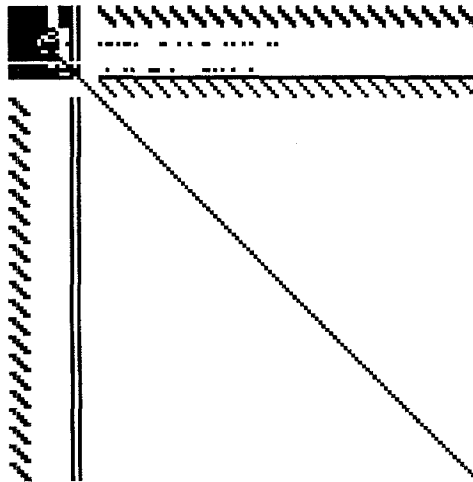


Figure 6. The pattern of nonzeros in the matrix `arc130.rua` ( $130 \times 130$ ), revealing an arrowhead pattern.

## 5. GENERALIZED MAT/VEC

The problem at hand is to multiply an  $n \times n$  matrix  $M = (m_{i,j})_{n \times n}$  and an  $n$ -vector  $x = (x_j)_{n \times 1}$  to produce as result, an  $n$ -vector  $y = (y_i)_{n \times 1}$ . Let  $\{\Psi_1, \Psi_2, \dots, \Psi_k\}$  be the staircase cover of  $M$  constructed by SCA (described in Section 3). From the proof of Theorem 4, it follows that  $\Psi_\ell <_\gamma \Psi_{\ell-1}$ , for all  $\ell$ ,  $2 \leq \ell \leq k$ . As generalized MAT/VEC is described, it will become clear that for our algorithm to work the staircases have to be totally ordered by  $<_\gamma$ . Generalized

MAT/VEC uses  $k$  PEs, each PE having six input ports, labeled  $I_1$ ,  $I_2$ ,  $I_3$ ,  $I_4$ ,  $I_5$ , and  $I_6$ , and two output ports, labeled  $O_1$  and  $O_2$ . A typical PE in generalized MAT/VEC is shown in Figure 7(a). The  $k$  PEs are labeled 1 through  $k$  and are connected in a linear array as shown in Figure 7(b). The components of the  $x$ -vector are fed from the right of generalized MAT/VEC through input port  $I_1$  of the PE labeled 1, in the order  $x_1, x_2, \dots, x_n$ . The components of the  $y$ -vector, initialized to 0, are fed from the left of generalized MAT/VEC, through input port  $I_2$  of the PE labeled  $k$ , in the order  $y_1, y_2, \dots, y_n$ . The product  $M \cdot x$  is accumulated in  $y$ , that is, when  $y_i$  exits PE 1, it contains the value  $\sum_{j=1}^n m_{i,j} x_j$ . The elements of each staircase  $\Psi_\ell$ , where,  $1 \leq \ell \leq k$ , are fed into the PE labeled  $\ell$  in increasing order of  $\leq_{se}$ . In particular, if  $(i, j) \in \Psi_\ell$ , then  $m_{i,j}$  is fed into input port  $I_3$ ,  $i$  is fed into input port  $I_5$ , and  $j$  is fed into input port  $I_4$  of the PE labeled  $\ell$ . Thus, along with an entry  $m_{i,j}$  of  $M$ , the row index  $i$  and the column index  $j$  are also fed to the PE. Since a staircase is fed into a PE in increasing order of  $\leq_{se}$ , the sequence of values fed into port  $I_4$  (the  $j$  values) and the sequence of values fed into port  $I_5$  (the  $i$  values) are both nondecreasing. Once PE  $\ell$  has  $m_{i,j}$  on its input port  $I_3$ , it then waits for  $x_j$  and  $y_i$  to appear on input ports  $I_1$  and  $I_2$ , respectively, and when they do appear, it updates  $y_i$  according to  $y_i := y_i + m_{i,j} \cdot x_j$ . The value fed into a PE via input port  $I_6$  depends on the relationship between the current input on  $I_3$  and the next input on  $I_3$ . If the next input on  $I_3$  is a matrix element that is in the same row as the current input, then  $I_6$  has the value  $h$  (horizontal). If the next input on  $I_3$  is a matrix element that is in the same column as the current input, then  $I_6$  has the value  $v$  (vertical). Otherwise  $I_6$  has the value  $d$  (diagonal).

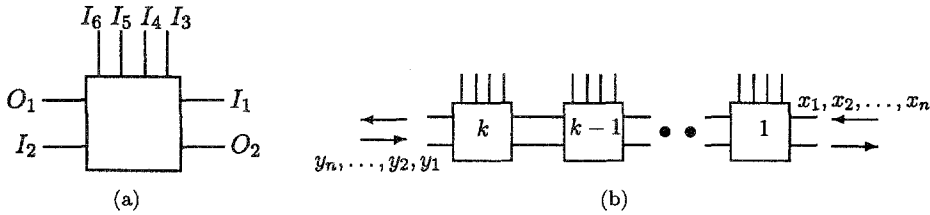


Figure 7. Sparse matrix-vector multiplication systolic network.

---

```

Step 1:   $R_m := [I_3]; R_j := [I_4]; R_i := [I_5];$ 
Step 2:  While  $(C_x < R_j)$  or  $(C_y < R_i)$  do
Step 2.1  if  $(\text{not empty}(I_1))$  and  $(C_x < R_j)$  then
            $\{R_x := [I_1]; C_x := C_x + 1;$ 
           if  $(C_x < R_j)$  then  $O_1 := R_x;$ 
Step 2.2  if  $(\text{not empty}(I_2))$  and  $(C_y < R_i)$  then
            $\{R_y := [I_2]; C_y := C_y + 1;$ 
           if  $(C_y < R_i)$  then  $O_2 := R_y;$ 
Step 3:   $R_y := R_y + R_m \cdot R_x$ 
Step 4:  if  $([I_6] = h)$  then  $\{O_1 := R_x\}$ 
           else if  $([I_6] = v)$  then  $\{O_2 := R_y\}$ 
           else  $\{O_1 := R_x; O_2 := R_y\}$ 

```

---

Figure 8. Program for each PE.

Each PE in the network executes the program shown in Figure 8 repeatedly until  $M \cdot x$  has been computed. Each PE has five internal registers,  $R_m$ ,  $R_i$ ,  $R_j$ ,  $R_x$ , and  $R_y$  and two counters  $C_x$  and  $C_y$ . The counters  $C_x$  and  $C_y$  are initialized to 0 and represent the index of the most recently received components of the  $x$ -vector and  $y$ -vector, respectively. Consider a PE labeled  $\ell$  for some  $\ell$ ,  $1 \leq \ell \leq k$ . After receiving  $m_{i,j}$ ,  $i$ , and  $j$  into registers  $R_m$ ,  $R_i$ , and  $R_j$ , respectively, (Step 1), the PE waits for the appropriate components of the  $x$ -vector ( $x_j$ ) and the  $y$ -vector ( $y_i$ ) to appear on input ports  $I_1$  and  $I_2$ , respectively, (Step 2). More precisely, the PE first checks

input port  $I_1$  (Step 2.1) and then checks input port  $I_2$  (Step 2.2) for input. Step 2.1 can be explained as follows. If the PE has not already received the correct component of the  $x$ -vector, that is, if  $C_x < R_j$ , and if there is some input, on input port  $I_1$ , then the input is copied into register  $R_x$  and the corresponding counter  $C_x$  is incremented. If  $C_x$  is still smaller than  $R_j$ , then the PE has no use for the component of the  $x$ -vector just received, and therefore, this component is moved to the output port  $O_1$ . Step 2.2 is similar to Step 2.1, except that a component of the  $y$ -vector is received as input. Step 2 terminates when  $C_x = R_j$  and  $C_y = R_i$ . Thus, for any PE,  $C_x$  (respectively,  $C_y$ ) keep track of the number of components of  $x$  (respectively,  $y$ ) that have reached the PE. Hence, when Step 2 is completed the correct components of the  $x$ -vector and  $y$ -vector have been received. On receiving  $x_j$  and  $y_i$ , the PE updates  $y_i$  according to  $y_i := y_i + m_{i,j} \cdot x_j$  (Step 3). In Step 4, the PE decides whether to retain either  $x_j$  or  $y_i$  for future use. In particular, if the next element in the staircase is in the same row as the current element, that is,  $[I_6] = h$ , then  $y_i$  is retained and  $x_j$  is passed on to the left neighbor (PE  $\ell + 1$ ). If the next element in the staircase is in the same column as the current element, that is,  $[I_6] = v$ , then  $x_j$  is retained and  $y_i$  is passed on to the right neighbor (PE  $\ell - 1$ ). If neither is true ( $[I_6] = d$ ), then both  $x_j$  and  $y_i$  are passed on to the left and right neighbor, respectively.

The main difference between the program executed by each PE in generalized MAT/VEC and the program executed by each PE in MAT/VEC is in Step 4. In MAT/VEC, each stripe in a stripe cover is fed into a distinct PE and after  $y_i$  is updated (as in Step 3), both  $x_j$  and  $y_i$  are passed on to the neighboring PEs, while in generalized MAT/VEC whether  $x_j$  or  $y_i$  (or both) is (are) passed on to the neighboring PE(s) depends on whether the next matrix element to be fed into the PE is in the same row or column as the current one. Note that generalized MAT/VEC is a generalization of MAT/VEC in the sense that a stripe may be fed into a PE and if so  $I_6$  will always have the value  $d$ .

Each connection between a pair of adjacent PEs can be thought of as a queue with capacity  $n$ . The reader may be concerned about this requirement; specifically, that the queue capacity grows linearly in the array size. Section 8 addresses this concern by explaining how a staircase cover can be constructed that accommodates a constant upper bound on queue capacities. For example, the connection between port  $O_1$  of PE  $\ell$  and port  $I_1$  of PE  $\ell + 1$  is a queue into which components of the  $x$ -vector are enqueued by PE  $\ell$  and dequeued by PE  $\ell + 1$ . The net result is that each PE has access to four queues: two queues (at input ports  $I_1$  and  $I_2$ ) that it can dequeue elements from and two queues (at the output ports  $O_1$  and  $O_2$ ) that it can enqueue into. For the purpose of our analysis, we give these queues names. The input queue for PE  $\ell$  that contains components of the  $x$ -vector (respectively,  $y$ -vector) will be called  $IQ_x(\ell)$  (respectively,  $IQ_y(\ell)$ ). Accordingly, the output queues will be called  $OQ_x(\ell)$  and  $OQ_y(\ell)$ . Note that  $IQ_x(\ell + 1)$  and  $OQ_x(\ell)$  are identical and likewise  $IQ_y(\ell)$  and  $OQ_y(\ell + 1)$  are identical for all  $\ell$ ,  $1 \leq \ell \leq k - 1$ . For notational convenience, we will use  $IQ_x(k + 1)$  as an alternate name for  $OQ_x(k)$  and  $IQ_y(0)$  as an alternate name for  $OQ_y(1)$ .

Since generalized MAT/VEC is systolic, the PEs execute their programs at different speeds depending upon the availability of data. To analyze the number of time steps required by generalized MAT/VEC, we focus on the slowest PE. To be precise, we introduce a hypothetical global synchronization scheme as suggested by Melhem. Replace Step 3 in Figure 8 by the following:

Step 3: Wait for a synchronization signal SYNC;  
 $R_y := R_y + R_m \cdot R_x$ ;

The purpose of the synchronization signal SYNC is to force the execution of generalized MAT/VEC into two alternating phases: a *communications phase* and a *processing phase*. During the communications phase data flows through the network until each PE is either waiting for data (in Step 2), or waiting for SYNC (in Step 3). We assume that all the PEs are connected to a hypothetical controller that issues the signal SYNC after detecting the termination of the

communications phase. At the instant SYNC is received, all PEs that are waiting in Step 3 perform the computation  $R_y := R_y + R_m \cdot R_x$ , while the other PEs remain idle. This is the processing phase. A communications phase followed by a processing phase is called a *global cycle* of the network. We measure the time taken by generalized MAT/VEC to compute  $M \cdot x$  by the number of global cycles required. We denote by  $CP_t$  and  $PP_t$ , the communications phase and the processing phase, respectively, in global cycle  $t$ . Note that the above synchronization scheme is hypothetical and simply serves as a way of defining a measure on the amount of time required for generalized MAT/VEC to compute the matrix-vector product. Furthermore, since this is the same measure of time used by Melhem [3], the comparison between the two schemes is made on the same basis.

|   |   |   |   |   |
|---|---|---|---|---|
|   |   | 1 | 1 |   |
| 2 | 2 | 2 | 1 |   |
|   | 3 |   | 1 |   |
|   | 3 | 2 |   | 1 |

Figure 9. A matrix with staircase width 3.

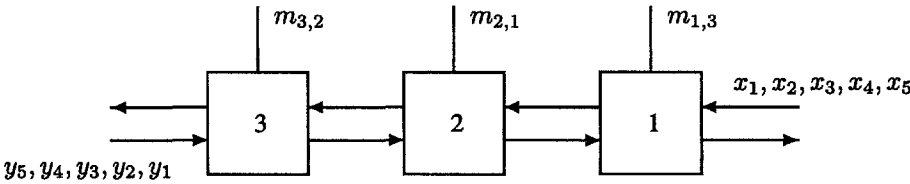


Figure 10. Initial status of generalized MAT/VEC.

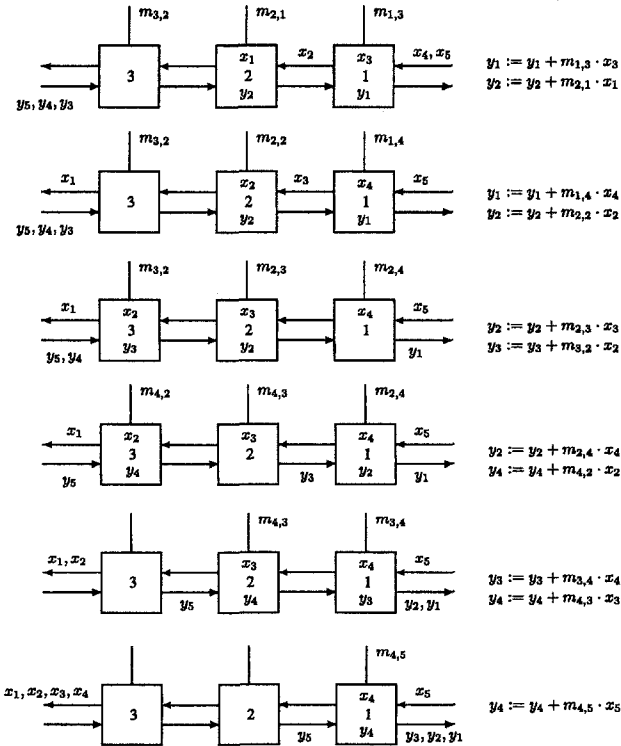


Figure 11. The computations performed by generalized MAT/VEC.

Figures 9–11 illustrate how generalized MAT/VEC performs a matrix-vector multiplication. Figure 9 illustrates a  $5 \times 5$  matrix whose staircase width is 3. The nonzero elements covered by  $\Psi_1$  are labeled 1, those covered by  $\Psi_2$  are labeled 2, and those covered by  $\Psi_3$  are labeled 3. Note that  $\Psi_3 <_\gamma \Psi_2 <_\gamma \Psi_1$ . Figure 10 shows the status of generalized MAT/VEC initially and Figure 11 shows the six global cycles that generalized MAT/VEC goes through in order to perform the matrix-vector multiplication. For each global cycle, the status of generalized MAT/VEC after the communications phase and the computations performed during the corresponding processing phase are shown. Notice that during global cycle 1, components  $x_1$  and  $x_2$  are both placed in queue  $IQ_x(2)$ . It is easy to see that the stripe width of the matrix shown in Figure 9 is six. Thus, MAT/VEC uses six PEs and the reader is invited to verify that MAT/VEC performs the same computations as generalized MAT/VEC, in each processing phase.

## 6. CORRECTNESS OF GENERALIZED MAT/VEC

The proof of correctness of generalized MAT/VEC depends fundamentally on two properties of our scheme that are established below (Lemmas 5 and 6). The first property is that, for all  $i$ ,  $y_i$  does exit generalized MAT/VEC. In other words, generalized MAT/VEC does not deadlock. In order to prove this, we first need to formalize the notion of a deadlock. Generalized MAT/VEC is said to be in a *deadlock* if for some PE  $k_1$ ,  $[I_4] = j_1$ ,  $[I_5] = i_1$ , and for some PE  $k_2$ ,  $[I_4] = j_2$ , and  $[I_5] = i_2$ , such that  $k_1 > k_2$ ,  $i_1 \leq i_2$ , and  $j_1 \geq j_2$ . The implication of the above condition is that PE  $k_1$  is waiting for  $x_{j_1}$  which is blocked by PE  $k_2$ , which in turn is waiting for  $y_{i_2}$ , which is blocked by PE  $k_1$ . A deadlock state is illustrated in Figure 12. The fact that staircases are totally ordered according to  $\leq_\gamma$  is crucial in ensuring that generalized MAT/VEC does not deadlock.

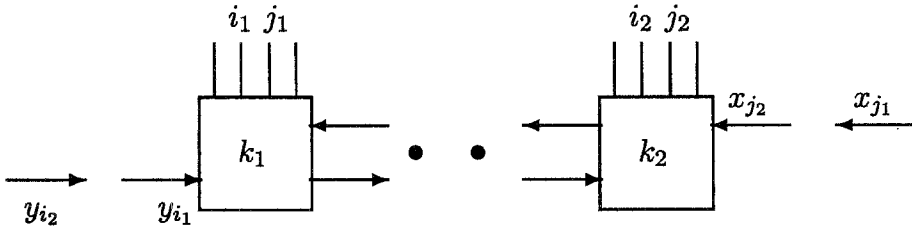


Figure 12. Generalized MAT/VEC in a deadlock state.

**LEMMA 5.** *Generalized MAT/VEC does not reach a deadlock.*

**PROOF.** To show this, we assume that generalized MAT/VEC reaches a deadlock state and obtain a contradiction. Because  $\Psi_{k_1} <_\gamma \Psi_{k_2}$ , it follows from the definition of  $<_\gamma$  that  $(i_1, j_1) <_{\text{sne}} (i_3, j_3)$  for some  $(i_3, j_3) \in \Psi_{k_2}$ . Since,  $i_1 \leq i_2$  and  $j_1 \geq j_2$ ,  $(i_2, j_2) \leq_{\text{sne}} (i_1, j_1)$ . By, transitivity of  $\leq_{\text{sne}}$  we have  $(i_2, j_2) <_{\text{sne}} (i_3, j_3)$ , which is a contradiction because  $(i_2, j_2)$  and  $(i_3, j_3)$  belong to the same staircase. ■

We now know that all  $y_i$  exit the systolic array; we do not know that each  $y_i$  has the correct value. To establish this we show a second property of our algorithm, which is that, when  $m_{i,j}$  reaches a PE,  $x_j$  and  $y_i$  have not traveled past the PE, and therefore, will participate in the computation  $y_i := y_i + m_{i,j} \cdot x_j$  eventually. This implies that when  $y_i$  exits the system, it contains the value  $\sum_{j=1}^n m_{i,j} \cdot x_j$ .

**LEMMA 6.** *For any PE  $\ell$ ,  $1 \leq \ell \leq k$ , just before the execution of Step 2 in the program shown in Figure 8, the following holds:*

$$C_x \leq R_j \quad \text{and} \quad C_y \leq R_i.$$

**PROOF.** The proof is by induction on the number of times Step 2 has already been executed by PE  $\ell$ .

BASE CASE. Suppose that Step 2 has been executed 0 times by PE  $\ell$ . Due to initialization,  $C_x = 0$  and  $C_y = 0$ . After Step 1 has been executed,  $R_i$  and  $R_j$  acquire values in  $J_n$ . Thus, after Step 1 has been executed and just before Step 2 is executed the first time, it is the case that  $C_x < R_j$  and  $C_y < R_i$ .

INDUCTION CASE. Assume that for some integer  $p \geq 0$ , the lemma holds after Step 2 has been executed  $p$  times and just before it is executed for the  $(p+1)^{\text{th}}$  time. We now show if PE  $\ell$  executes Step 2 for the  $(p+2)^{\text{nd}}$  time, then just before this execution of Step 2, Lemma 2 holds. Two cases are possible depending on whether the condition in Step 2 evaluates to true or false when Step 2 is executed for the  $(p+1)^{\text{th}}$  time.

Case 1. Suppose that the condition  $(C_x < R_j)$  or  $(C_y < R_i)$  evaluates to true when Step 2 is executed the  $(p+1)^{\text{th}}$  time. In the body of the loop (Steps 2.1 and 2.2)  $C_x$  is incremented by at most one, if  $C_x < R_j$  and  $C_y$  is incremented by at most one, if  $C_y < R_i$ . In any case, just before Step 2 is executed for the  $(p+2)^{\text{nd}}$  time, we have  $C_x \leq R_j$  and  $C_y \leq R_i$ .

Case 2. Suppose that the condition  $(C_x < R_j)$  or  $(C_y < R_i)$  evaluates to false when Step 2 is executed the  $(p+1)^{\text{th}}$  time. By the induction hypothesis, we have  $C_x = R_j$  and  $C_y = R_i$ . The steps executed immediately after Step 2 are Steps 3 and 4 and these steps do not change the value of  $C_x$  and  $C_y$ . When the PE finishes the execution of Step 4, it begins again at Step 1. If there is more input on  $I_3$ , then in Step 1,  $R_i$  and  $R_j$  get new values, but these new values are greater than or equal to the corresponding old values. This is because the elements fed into PE  $\ell$  belong to  $\Psi_\ell$  and are fed in increasing order according to  $\leq_{se}$ . Hence, just before Step 2 is executed for the  $(p+2)^{\text{nd}}$  time  $C_x \leq R_j$  and  $C_y \leq R_i$ .

By induction, the lemma follows. ■

It is easy to see that for any PE  $\ell$ ,  $1 \leq \ell \leq k$ ,  $C_x$  is the number of components of the vector  $x$  that have reached the PE. Similarly, it is easy to see that  $C_y$  is the number of components of the vector  $y$  that have reached the PE. Thus, Lemma 6 implies that when  $m_{i,j}$  reached PE  $\ell$ , the components  $x_j$  and  $y_i$  have not already traveled past the PE. Since, Lemma 5 shows that generalized MAT/VEC does not deadlock, eventually the components  $x_j$  and  $y_i$  will reach PE and the computation  $y_i := y_i + m_{i,j} \cdot x_j$  is performed. This implies the correctness of generalized MAT/VEC, as stated in the following theorem.

**THEOREM 7.** *For each  $i$ ,  $1 \leq i \leq n$ ,  $y_i$  exits at output port  $O_2$  of the rightmost PE in the array with value  $\sum_{j=1}^n m_{i,j} \cdot x_j$ .*

## 7. PERFORMANCE OF GENERALIZED MAT/VEC

In this section, we analyze the running time of generalized MAT/VEC relative to the running time of MAT/VEC. As mentioned before, to compute  $M \cdot x$ , generalized MAT/VEC requires STAIR( $M$ ) PEs, while MAT/VEC requires STRIPE( $M$ ) PEs. For any  $M$  we have  $\text{STAIR}(M) \leq \text{STRIPE}(M)$  and the experiments in Section 4 indicate that generalized MAT/VEC often has a significantly smaller hardware requirement. In the main result in this section, we show that, despite having a smaller hardware requirement, generalized MAT/VEC requires the same time (number of global cycles) as does MAT/VEC. We use the notion of a global cycle as our unit of time for ease of analysis and for appropriateness of comparison. At the end of this section we mention that even if we had used another, possibly more realistic measure of time, we would have concluded that generalized MAT/VEC is at least as fast as MAT/VEC.

### 7.1. Counting Global Cycles

Define inductively a sequence of position index sets  $CF_1, CF_2, CF_3, \dots$ , as follows:

$$\Gamma_0 = \Gamma,$$

and, for all  $i \geq 1$ ,

$$\begin{aligned} CF_i &= \text{set of minimal elements of } (\Gamma_{i-1}, \leq_{se}), \\ \Gamma_i &= \Gamma_{i-1} - CF_i. \end{aligned}$$

Each  $CF_i$  is called a *computational front*. For the matrix in Figure 9,

$$\begin{aligned} CF_1 &= \{(1, 3), (2, 1)\}, & CF_4 &= \{(4, 2), (2, 4)\}, \\ CF_2 &= \{(1, 4), (2, 2)\}, & CF_5 &= \{(3, 4), (4, 3)\}, \\ CF_3 &= \{(2, 3), (3, 2)\}, & CF_6 &= \{(4, 5)\}. \end{aligned}$$

Note that a computational front is a chain in the poset  $(\Gamma, \leq_{sne})$ . Melhem [3] shows that elements in each computational front participate in a computation in each processing phase. In other words, Melhem shows that MAT/VEC performs the computation  $y_i := y_i + m_{i,j} \cdot x_j$  in processing phase  $PP_t$  if and only if  $(i, j) \in CF_t$ . Theorem 8 shows that the same is true for the computations performed by generalized MAT/VEC. The implication, of course, is that MAT/VEC and generalized MAT/VEC perform the same computations in each global cycle.

**THEOREM 8.** *For all  $t$ ,  $(i, j) \in CF_t$  if and only if the computation  $y_i := y_i + m_{i,j} \cdot x_j$  is performed in processing phase  $PP_t$  by generalized MAT/VEC.*

**PROOF.** For the convenience of argument, let  $CF_0 = \emptyset$  and let  $PP_0$  be a dummy processing phase in which no computations are performed. The proof of the theorem is by induction on  $t$ .

**BASE CASE.** The claim is trivially true when  $t = 0$  because of the definitions of  $CF_0$  and  $PP_0$ .

**INDUCTION CASE.** Let  $t \geq 1$  and assume that, for all  $t' \leq t-1$ , we have  $(i', j') \in CF_{t'}$  if and only if generalized MAT/VEC performs the computation  $y_{i'} := y_{i'} + m_{i',j'} \cdot x_{j'}$  in  $PP_{t'}$ . Using this induction hypothesis, we show that  $(i, j) \in CF_t$  if and only if generalized MAT/VEC performs the computation  $y_i := y_i + m_{i,j} \cdot x_j$  in  $PP_t$ . Let

$$\Gamma_\ell = \Gamma - (CF_1 \cup CF_2 \cup \dots \cup CF_\ell),$$

for all  $\ell \geq 0$ . Let us focus on the status of generalized MAT/VEC just after  $PP_{t-1}$ . Let  $(i, j) \in CF_t \cap \Psi_p$  for some  $p$ ,  $1 \leq p \leq k$ . By the induction hypothesis,  $m_{i,j}$  has not yet been used in a computation. By definition of  $CF_t$ ,  $(i, j)$  is a minimal element with respect to  $\leq_{se}$  in  $\Gamma_{t-1}$ . Hence,  $m_{i,j}$  is the  $I_3$ -input to the PE labeled  $p$  in global cycle  $t$ . We will now show that during  $CP_t$ , the components  $x_j$  and  $y_i$  reach PE  $p$ , and thus, the PE computes  $y_i := y_i + m_{i,j} \cdot x_j$  in  $PP_t$ .

By Lemma 6, we know that  $y_i$  is in queue  $IQ_y(p_L)$ , where  $p_L \geq p$ , and  $x_j$  is in queue  $IQ_x(p_R)$ , where  $p_R \leq p$ . We first show that for all PEs to the left of PE  $p$ ,  $[I_5] > i$ , implying that  $y_i$  is not blocked by any PE to the left of PE  $p$  and reaches PE  $p$  in  $CP_t$ . The proof is by contradiction. Suppose that there is a PE labeled  $p' > p$  (that is, to the left of PE  $p$ ) for which  $[I_5] \leq i$ . Specifically, assume that for PE  $p' > p$ ,

$$[I_5] = i', \quad [I_4] = j', \quad i' \leq i.$$

Then,  $j' > j$ , because otherwise if  $j' \leq j$ , then  $(i', j') \leq_{se} (i, j)$  and  $(i, j)$  is not a minimal element of  $\Gamma_{t-1}$  with respect to  $\leq_{se}$ . Thus, we have

$$i' \leq i \quad \text{and} \quad j' > j. \tag{1}$$

Since  $p' > p$ , we know that  $\Psi_{p'} \leq_\gamma \Psi_p$ . Hence, by the definition of  $\leq_\gamma$ , there is a position index  $(i'', j'') \in \Psi_p$ , such that  $(i', j') <_{sne} (i'', j'')$ . In other words,

$$i' > i'' \quad \text{and} \quad j' < j''. \tag{2}$$

But, (1) and (2) together imply that  $(i, j) <_{\text{sne}} (i'', j'')$ . This is a contradiction because  $(i, j)$  and  $(i'', j'')$  both belong to the same staircase  $\Psi_p$ . Hence, for every PE to the left of PE  $m$ ,  $[I_5] > i$ . This allows  $y_i$  to reach PE  $p$  in  $CP_t$ . A similar argument suffices to show that for all PEs to the right of PE  $p$ ,  $[I_4] > j$ , thus allowing  $x_j$  to reach PE  $p$  in  $CP_t$ . Hence,  $y_i := y_i + m_{i,j} \cdot x_j$  is computed in  $PP_t$ .

To complete the proof we need to show that if  $(i, j) \notin CF_t$  then  $y_i := y_i + m_{i,j} \cdot x_j$  is not computed in  $PP_t$ . Suppose  $(i, j) \in CF_{t'}$  for some  $t' < t$ ; by the induction hypothesis  $m_{i,j}$  has already participated in a computation and will not participate in any further computations. So assume that  $(i, j) \in CF_{t'}$  for some  $t' > t$ . This implies that  $(i, j) \in \Gamma_{t-1}$ . Now let us be more specific and assume that  $(i, j) \in \Gamma_{t-1} \cap \Psi_p$  for some  $p$ ,  $1 \leq p \leq k$ . There are two cases depending on whether  $(i, j)$  is a minimal position index in  $\Gamma_{t-1} \cap \Psi_p$  with respect to  $\leq_{\text{se}}$ .

CASE 1. If  $(i, j)$  is not the minimal position index in  $\Gamma_{t-1} \cap \Psi_p$ , then  $m_{i,j}$  is not the  $I_3$ -input to PE  $p$  in global cycle  $t$ , and hence, the computation  $y_i := y_i + m_{i,j} \cdot x_j$  is not performed in  $PP_t$ .

CASE 2. Suppose that  $(i, j)$  is the minimal position index in  $\Gamma_{t-1} \cap \Psi_p$ . Since  $(i, j) \notin CF_t$ , there is a position index  $(i', j') \in \Gamma_{t-1}$ , such that  $(i', j') \leq_{\text{se}} (i, j)$ . Now suppose that  $(i', j') \in \Psi_{p'}$  for some  $p' \neq p$ . If  $p' > p$ , then PE  $p'$  is to the left of PE  $p$ . By Lemma 6, component  $y_{i'}$  is to the left of PE  $p'$  and since  $i \geq i'$ , component  $y_i$  is also to the left of PE  $p'$ . Thus,  $y_i$  is blocked by PE  $p'$  and cannot reach PE  $p$  in  $CP_t$ . Similarly, it can be shown that if  $p' < p$ , then  $x_j$  is blocked by some PE to the right of PE  $p$  and cannot reach PE  $p$  in  $CP_t$ . This implies that as claimed,  $y_i := y_i + m_{i,j} \cdot x_j$  is not computed in  $PP_t$ .

By induction, the theorem follows. ■

Melhem provides a lower bound (see Proposition 3.1 in [3]) and an upper bound (see Proposition 3.2 in [3]) on the number of global cycles that MAT/VEC requires to complete  $M \cdot x$ . Neither of the bounds is tight, and he leaves the precise characterization of the number of global cycles required by MAT/VEC an open question. The following theorem provides the precise number of global cycles required by generalized MAT/VEC (and MAT/VEC) to compute  $M \cdot x$ , as a function of how the nonzeros are distributed in matrix  $M$ .

**THEOREM 9.** *Let  $\Psi$  be a largest staircase in  $M$ . Then, the number of global cycles required by generalized MAT/VEC or MAT/VEC to compute  $M \cdot x$  is  $|\Psi|$ .*

**PROOF.** Let  $CF_1, CF_2, \dots, CF_T$  be the nonempty computational fronts of  $M$ . From the definition of computational fronts, it is easy to see that there is a sequence

$$(i_1, j_1) \leq_{\text{se}} (i_2, j_2) \leq_{\text{se}} \dots \leq_{\text{se}} (i_T, j_T),$$

such that  $(i_p, j_p) \in CF_p$ , for  $1 \leq p \leq T$ . The above sequence is an antichain in  $(\Gamma, \leq_{\text{sne}})$ . This implies that  $CF_1, CF_2, \dots, CF_T$  is a smallest set of chains in  $(\Gamma, \leq_{\text{sne}})$  covering  $\Gamma$ . Therefore, by Theorem 1,  $T$  is equal to the size of a largest antichain in  $(\Gamma, \leq_{\text{sne}})$ . An antichain in  $(\Gamma, \leq_{\text{sne}})$  is a staircase, all of whose elements belong to  $\Gamma$ . The theorem follows. ■

In the matrix shown in Figure 9, the size of the largest staircase is six. This is equal to the number of computational fronts in the matrix, and is therefore, equal to the number of global cycles required by generalized MAT/VEC and MAT/VEC.

## 7.2. Counting Clock Pulses

The reader may be concerned that using a global cycle as a unit of time ignores the amount of communication among PEs that has to go on between consecutive processing phases. An alternative approach is to count the number of *clock pulses* required to complete the task, assuming that at each clock pulse, each PE performs a read-compute-write cycle. More precisely, at each clock pulse, each PE reads the input ports that it is expecting input on, performs a computation if it has the requisite data, and then writes data that it no longer needs on output ports. It



is possible to show that for any matrix  $M$  the number of clock pulses required by generalized MAT/VEC is no greater than the number of clock pulses required by MAT/VEC. The proof of this claim is more tedious than the proof of the corresponding claim for global cycles and is not included here. We merely present an example to provide insights into the situation. In Figure 13 a  $3 \times 3$  matrix is shown with a staircase cover of width 2 on the left and a stripe cover of width 4 on the right. The blank slots correspond to zeroes; entry  $i$  belongs to the  $i^{\text{th}}$  staircase or stripe. Figure 14 shows the matrix-vector multiplication performed on this matrix by generalized MAT/VEC and organized by clock pulses. Since the matrix is covered by two staircases, we have two PEs. Each row in the picture corresponds to the array of two PEs at a particular clock pulse. Each cell corresponds to a PE. The entry at the top of each cell denotes the position indices of the next matrix element, the entry at the left denotes the index of the next element of the  $y$ -vector, and the entry at the right denotes the index of the next element of the  $x$ -vector. An empty input port is denoted by \*. Shaded cells represent PEs and clock pulses where actual computation (as opposed to mere communication) took place. For example, in clock pulse 4, PE 1 had data  $m_{1,3}$ ,  $y_1$ , and  $x_3$  and performed the computation  $y_1 \leftarrow y_1 + m_{1,3} \cdot x_3$ . At that clock pulse, PE 2 is unable to perform any computation because it is missing  $y_3$ . It takes seven clock pulses for all the  $y_i$  to exit the array. Figure 15 shows the same matrix-vector multiplication performed by MAT/VEC. Four PEs are used because four stripes were required to cover the matrix (see Figure 13). Despite the additional PEs, MAT/VEC takes additional clock pulses (11 in all) to complete the computation. It can be shown by induction that at any clock

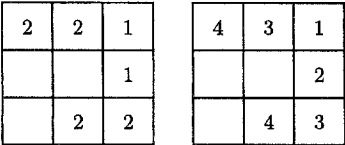


Figure 13. A  $3 \times 3$  matrix. On the left a staircase cover with width 2 is shown and on the right a stripe cover with width 4 is shown.

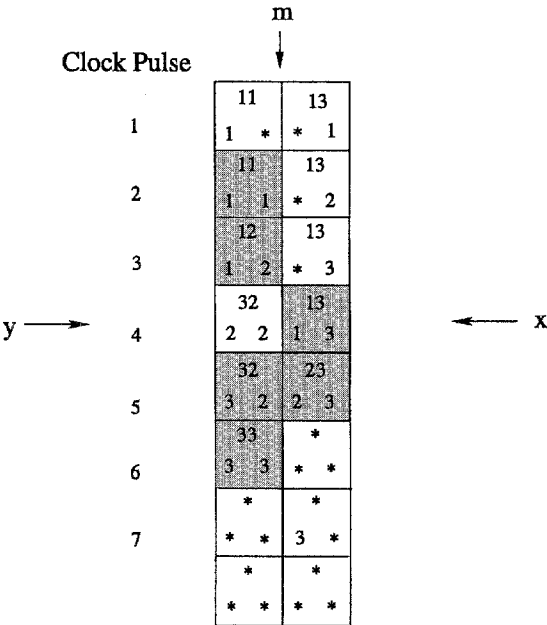


Figure 14. Computing a matrix-vector product on generalized MAT/VEC with two PEs.

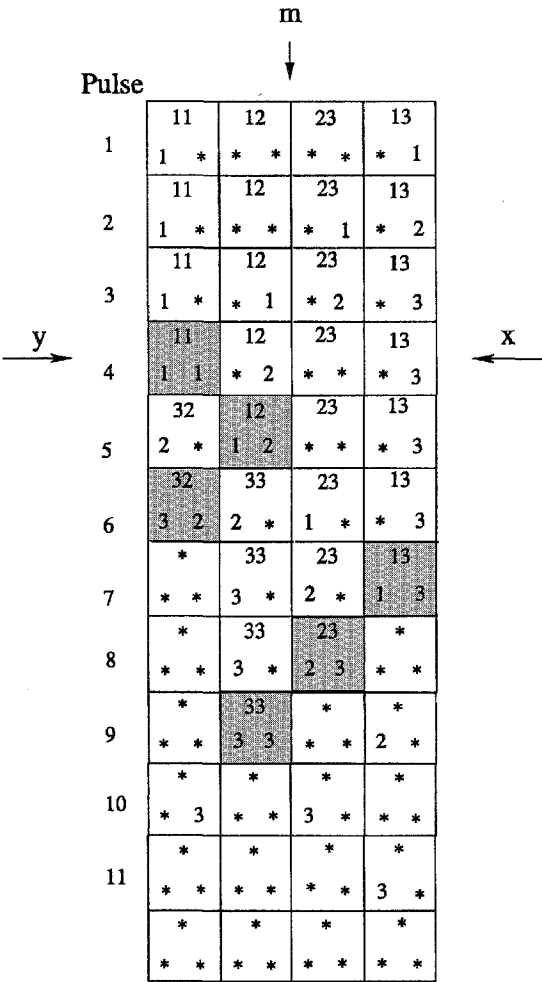


Figure 15. Computing a matrix-vector product on MAT/VEC with four PEs.

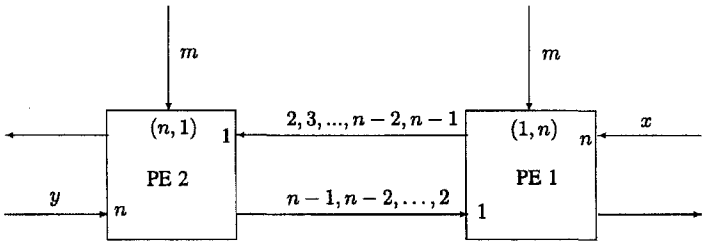


Figure 16. Each of the queue between the two PEs contains  $(n - 2)$  elements.

pulse, the computations completed by MAT/VEC is a subset of the computations completed by generalized MAT/VEC. The intuition is that because of a larger array of PEs, elements have further to travel to reach the appropriate PE. This increases communication time and decreases parallelism.

### 8. FUTURE DIRECTIONS

In this paper, we have presented a natural generalization of the systolic array scheme proposed by Melhem [3] for matrix-vector multiplication. Our scheme, called generalized MAT/VEC outperforms MAT/VEC in that it has, typically a significantly smaller hardware requirement, without paying in extra time.

The reader may be concerned about the fact that generalized MAT/VEC assumes that PEs have access to unbounded queues. Since PEs are relatively simple pieces of hardware, this may seem unreasonable. For example, consider the “border matrix”  $M = (m_{i,j})_{n \times n}$  matrix, in which  $m_{i,j} \neq 0$  if and only if  $i \in \{1, n\}$  or  $j \in \{1, n\}$ . When  $M$  is processed by generalized MAT/VEC, we eventually reach the state shown in Figure 16 in which each of the two queues between PEs has  $(n - 2)$  elements in it.

This illustrates worst case behavior and in general queues need to be as large as the largest “step”—the number of elements belonging to a single row (or column)—in a staircase. If we are given a bound, say a constant bound  $k$ , on queue size, then our strategy would be to partition the positions of nonzero entries in the matrix into  $k$ -staircases, which are staircases which contains at most  $k$  elements from a row or a column. This will ensure that all queues need to hold at most  $k$  elements at any time during the algorithm. Finding a minimum width covering of a matrix by  $k$ -staircases is as easy as finding a minimum width staircase cover. As  $k$  increases, larger queues are possible, but the width of a minimum  $k$ -staircase cover decreases. The extremes are familiar to us: when  $k = 1$  we have an instance of Melhem’s stripe covers and when  $k = n$ , we have an instance of the staircase covers as described in this paper. The precise nature of the trade-off between the value  $k$  and the width of  $k$ -staircases is not clear and might be an interesting future direction of research.

In Section 3, we presented SCA an algorithm for computing the staircase width of a matrix. We did not consider the issue of rearranging the rows or columns of the matrix to minimize staircase width. This problem, similar to the problem of minimizing bandwidth of a matrix, is NP-complete [31], but nothing is known about obtaining approximate solutions to this problem. This is another future direction of research that interests us.

Finally, as mentioned earlier, reconfigurable VLSI technology, especially FPGAs, provides the flexibility to implement a variable number of processing elements and queues of varying sizes in fast hardware. Mapping staircase-based algorithms to pipelined FPGA bus systems is an interesting challenge for the engineer.

## REFERENCES

1. E.-J. Im and K. Yelick, Optimizing sparse matrix kernels for data mining, *SIAM International Conference on Data Mining*, <http://www.cs.berkeley.edu/~ejim/publication/>, (submitted).
2. E.-J. Im and K. Yelick, Optimizing sparse matrix vector multiplication for register reuse, *International Journal of High Performance Computing Applications (SCI)*, <http://www.cs.berkeley.edu/~ejim/publication/>, (submitted).
3. R. Melhem, Parallel solution of linear systems with striped sparse matrices, *Parallel Computing* **6**, 165–184, (1988).
4. I.S. Duff, Sparse numerical linear algebra: direct methods and preconditioning, In *The State of the Art in Numerical Analysis*, (York, 1996), pp. 27–62, Oxford Univ. Press, New York, (1997).
5. P.E. Bjørstad and T. Sørsvik, Data-parallel BLAS as a basis for LAPACK on massively parallel computers, In *Linear Algebra for Large Scale and Real-Time Applications*, (Leuven, 1992), pp. 13–20, Kluwer Acad. Publ., Dordrecht, (1993).
6. J. Dongarra, Performance of LAPACK, In *Large-Scale Matrix Problems and the Numerical Solution of Partial Differential Equations*, (Lancaster, 1992), pp. 55–67, Oxford Univ. Press, New York, (1994).
7. K.Y. Chen, Minimizing the bandwidth of sparse symmetric matrices, *Computing* **11**, 103–110, (1973).
8. J.-C. Luo, Algorithms for reducing the bandwidth and profile of a sparse matrix, *Computers & Structures. An International Journal* **44** (3), 535–548, (1992).
9. R. Melhem, Determination of stripe structures for finite element matrices, *SIAM Journal on Numerical Analysis* **24** (6), 1419–1433, (1987).
10. D.J. Evans, Block matrix multiplication and LU factorisation systolic arrays, *Int. J. Comput. Math.* **76** (1), 45–57, (2000).
11. P. Rózsa, *The Role of Mathematics in Modern Engineering*, (Melbourne, 1994), pp. 85–103, Studentlitteratur, Lund, (1996).
12. Y. Saad, ILUM: A multi-elimination ILU preconditioner for general sparse matrices, *SIAM J. Sci. Comput.* **17** (4), 830–847, (1996).
13. T.A. Davis and I.S. Duff, A combined unifrontal/multifrontal method for unsymmetric sparse matrices, *ACM Trans. Math. Software* **25** (1), 1–20, (1999).

14. J.W.H. Liu, The multifrontal method for sparse matrix solution: Theory and practice, *SIAM Rev.* **34** (1), 82–109, (1992).
15. W. Hackbusch, A sparse matrix arithmetic based on  $\mathcal{H}$ -matrices. I. Introduction to  $\mathcal{H}$ -matrices, *Computing* **62** (2), 89–108, (1999).
16. S.A. Sauter, Variable order panel clustering, *Computing* **64**, 223–261, (2000).
17. C.E. Leiserson, *Area-Efficient VLSI Computation*, MIT Press, Cambridge, MA, (1982).
18. A. DeHon, The density advantage of configurable computing, *Computer* **33**, 41–50, (2000).
19. K. Compton and S. Hauck, Reconfigurable computing: A survey of systems and software, *ACM Computing Surveys* **34**, 171–210, (2002).
20. M. Eisenring and M. Platzner, A framework for run-time reconfigurable systems, *Journal of Supercomputing* **21**, 145–159, (2002).
21. M. Platzner, Reconfigurable accelerators for combinatorial problems, *Computer* **33**, 58–61, (2000).
22. X.J. Zhang and K.W. Ng, A Review of high-level synthesis for dynamically reconfigurable FPGAs, *Microprocessors and Microsystems* **24**, 199–211, (2000).
23. K.Q. Li, Constant time Boolean matrix multiplication on a linear array with a reconfigurable pipelined bus system, *Journal of Supercomputing* **11**, 391–403, (1997).
24. K.Q. Li, Y. Pan and S.Q. Zheng, Fast and processor efficient parallel matrix multiplication algorithms on a linear array with a reconfigurable pipelined bus system, *IEEE Transactions on Parallel and Distributed Systems* **9**, 705–720, (1998).
25. W.T. Trotter, *Combinatorics and Partially Ordered Sets: Dimension Theory*, The Johns Hopkins University Press, Baltimore, MD, (1992).
26. R.P. Dilworth, A decomposition theorem for partially ordered sets, *Annals of Mathematics* **51**, 161–166, (1950).
27. L.S. Heath, F.T. Leighton and A.L. Rosenberg, Comparing queues and stacks as mechanisms for laying out graphs, *SIAM Journal of Discrete Mathematics* **5** (3), 398–412, (1992).
28. L.S. Heath and S.V. Pemmaraju, Stack and queue layouts of posets, *SIAM J. Discrete Math.* **10** (4), 599–625, (1997).
29. L.S. Heath and S.V. Pemmaraju and A.N. Trenk, Stack and queue layouts of directed acyclic graphs. I, *SIAM J. Comput.* **28** (4), 1510–1539, (1999).
30. L.S. Heath and S.V. Pemmaraju, Stack and queue layouts of directed acyclic graphs. II, *SIAM J. Comput.* **28** (5), 1588–1626, (1999).
31. L.S. Heath and A.L. Rosenberg, Laying out graphs using queues, *SIAM Journal of Computing* **21** (5), 927–958, (1992).
32. H.W. Lang, M. Schimmler, H. Schneck and H. Schroder, Systolic sorting on a mesh-connected network, *IEEE Transactions on Computers* **34** (7), 652–658, (1985).
33. S. Oliveira, A new parallel chasing algorithm for transforming arrowhead matrices to tridiagonal form, *Math. Comp.* **67** (221), 221–235, (1998).